Periodico di Mineralogia (2011), 80, 2, 287-307 DOI: 10.2451/2011PM0021

PERIODICO di MINERALOGIA
established in 1930

An International Journal of
MINERALOGY, CRYSTALLOGRAPHY, GEOCHEMISTRY, ORE DEPOSITS, PETROLOGY, VOLCANOLOGY
and applied topics on *Environment*, *Archeometry* and *Cultural Heritage*

Volcanic geology and petrology of the Val Calanna succession (Mt. Etna, Southern Italy): discovery of a new eruptive center

Eugenio Nicotra, Carmelo Ferlito, Marco Viccaro* and Renato Cristofolini

Dipartimento di Scienze Geologiche, Università di Catania, Corso Italia 57, I-95129, Catania, Italy
*Corresponding Author: *m.viccaro@unict.it*

Abstract

A new geological survey of the Val Calanna area at Mt. Etna (the southeastern extension of Valle del Bove, hereafter VdB), along with petrographic and geochemical data, highlighted some differences in the volcanic succession with respect to that previously reported in literature. Our study confirms that the most ancient volcano-stratigraphic Unit of the VdB crops out at Mt. Calanna, recently interpreted as a dyke swarm. The Mt. Calanna Unit is overlain by the 80-m-thick lava succession of the Salto della Giumenta Unit, one of the Ancient Alkaline Centers. Above this, volcanics of the Mt. Zoccolaro Unit constitute the frame of the present-day homonymous ridge. Mt. Zoccolaro lavas are benmoreites characterized by amphibole megacrysts, showing features similar to those of the Trifoglietto phase (100-60 ka). The eastern portion of the Mt. Zoccolaro edifice is overlain by the volcanic succession of a newly recognized small-sized eruptive Center: the Fior di Cosimo (FdC). The FdC Unit is constituted of a sequence of alternating lavas and pyroclastic deposits which dip radially away from an inferred vent hypothetically located in the middle of Val Calanna. Relationships between major oxides of FdC lavas and their stratigraphic position show an increasing degree of differentiation through time, from basalts to benmoreites. Simulations of crystal fractionation through MELTS revealed that the most evolved FdC lavas can be derived by subtraction of 32% of ~An_{66-82} plagioclase, 8% of augitic clinopyroxene, 8 wt% of spinel, 4% of ~Fo_{68-72} olivine and traces (< 1%) of apatite from a basaltic composition (54% of total solid fractionated). The proposed model for the FdC magmatic evolution is therefore the intrusion of a slightly differentiated magma at shallow crustal levels. Magma supply should have then ceased forming a reservoir that allowed differentiation by crystal fractionation, gradually leading to an increase of the volatile pressure of the system. This favored amphibole crystallization, as observed in the last-emitted products. The available data suggest that FdC can be attributed to a pre-Ellittico eruptive phase.

Key words: Valle del Bove; geological survey; magma differentiation; crystal fractionation; shallow feeding system.

Introduction

Since the beginning of its activity about 500 ka ago (Gillot et al., 1994; Branca et al., 2008), Mt. Etna has been characterized by the growth and destruction of several eruptive centers (cf. Romano, 1982; Branca et al., 2008). From the earliest researches into Mt. Etna geology, the steep and crumbly walls of Valle del Bove, carved on the eastern flank of the volcano, have offered an opportunity to expand our knowledge on the most ancient eruptive centers (e.g. Sartorius von Waltershausen, 1880; Romano, 1982; McGuire, 1982; Ferrari et al., 1989; Ferlito and Cristofolini, 1991; Calvari et al., 1994; Coltelli et al., 1994; D'Orazio et al., 1997; Branca et al., 2008; Ferlito and Nicotra, 2010). Understanding of the long-term evolution of magmas also leads to a more global view of Mt. Etna and its geodynamic framework. The multidisciplinary study of the evolution of a past eruptive center can offer new insights into the interpretation of current volcanic activity, and also suggest general models of magma evolution and eruptive behavior.

From this viewpoint, a multidisciplinary study was undertaken of the Val Calanna area, located at the south-eastern end of the Valle del Bove. Field evidence revealed a more complex geology than that provided by the literature (cf. Romano, 1982; Ferrari et al., 1989; Branca et al., 2008). The volcanic succession of Val Calanna is of particular importance in the study of the evolution of Mt. Etna given that the remains of several eruptive centers attributed to the first stages of alkaline activity crop out on its flanks. An appropriate position for the Mt. Calanna eruptive center within the Etnean succession has been an issue of debate for several years (Klerkx, 1970; Romano and Guest, 1979; McGuire, 1982; Romano, 1982; Ferrari et al., 1989; Ferlito and Nicotra, 2010), and many volcanological aspects are still unknown.

This study offers a new reconstruction of the Val Calanna succession based on a detailed geological survey and petrochemical data of volcanic rocks. The survey also revealed the occurrence of a deeply eroded edifice probably referring to a small volcanic center never previously recognized. The eruptive axis of this center may have been in the middle of the Val Calanna. The aims of the present paper are: 1) the definition of the volcano-stratigraphic succession of the Val Calanna within the frame of the Valle del Bove; 2) the characterization of the newly discovered Fior di Cosimo eruptive center; 3) the comprehension of the magmatic evolution of this center.

Geological and volcanological background

Mount Etna

Mount Etna (Eastern Sicily) is a Quaternary composite volcano extending over ~ 1250 km^2, which grew to its present elevation (~ 3340 m a.s.l.) through the accumulation of lavas and tephra erupted from various centers. The volcanic edifice is located at the edge of three regional domains (Figure 1A): the Hyblean Plateau, the Apennine-Maghrebian overthrust belt and the oceanic Ionian basin (Lentini, 1982; Cristofolini et al., 1979; Ben Avraham and Grasso, 1990). Furthermore, two important regional tectonic systems converge in the area of Mt. Etna, namely: the NNW-SSE Hyblean-Maltese fault system and the NNE-SSW Taormina-Messina alignment (cf. Monaco et al., 1997).

Early Etnean products, dating from 500 to 220 ka (Gillot et al., 1994; Branca et al., 2008 and references therein), are tholeiitic pillow lavas and hyaloclastites (Corsaro and Cristofolini, 1997) that later changed to subaerial tholeiitic and transitional basalts. The bulk of the Etnean edifice is constituted by Na-alkaline lavas and tephra erupted over the last 220 ka (Gillot et al., 1994; Viccaro and Cristofolini, 2008; Branca et al., 2008 and references therein).

The alkaline sequence is divided in four major

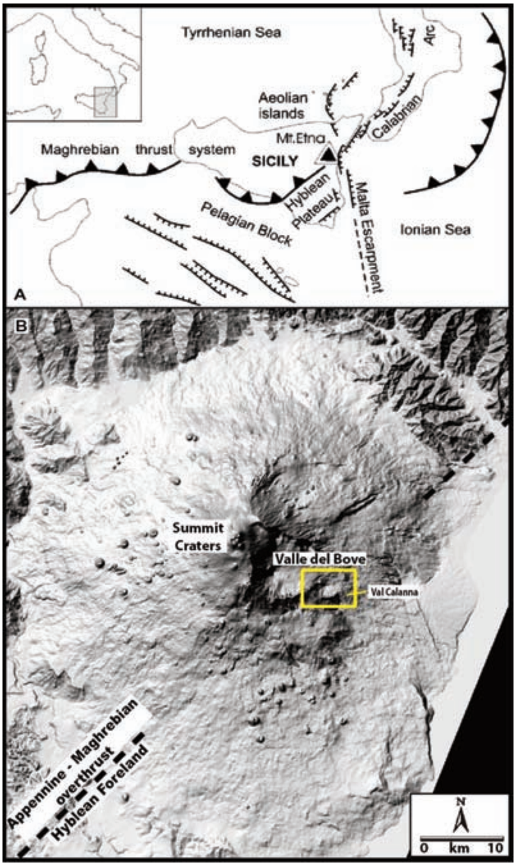

Figure 1. A) Structural and geodynamic framework of Southern Italy with the principal domains involved in active tectonics (modified after Monaco et al., 2005); B) Digital Elevation Model of Mt. Etna volcano (from Monaco et al., 2010).

volcano-stratigraphic units (Romano, 1982; VV.AA., 1982; Gillot et al., 1994): the Ancient Alkaline Centers (AAC, 220-100 ka), which include all the small- and modest-sized eruptive centers until the onset of the Trifoglietto; Trifoglietto (100-60 ka); Ellittico (or Ancient Mongibello; 60-15 ka) and Recent Mongibello (~ 15 ka to present). Recent research, based on the unconformity-bounded stratigraphic units (UBSU; Salvador, 1987; 1994) and $^{40}Ar/^{39}Ar$ dating, present a reconstruction of the Etnean alkaline activity in three main phases (Branca et al., 2004; 2008): 1) the Timpe phase (TI), developed along the Timpe Faults system (Ionian coast) and characterized by transitional products (220-120 ka); this phase also includes the Calanna volcano (~ 128 ka; Branca et al., 2008), which was attributed to the AAC by Romano (1982); 2) the Valle del Bove phase, consisting of several polygenic Na-alkaline eruptive centers (120-80 ka) whose products are concentrated in the Valle del Bove area; 3) the Stratovolcano phase (80 ka - present), to which belong the Ellittico (80-15 ka) and the Mongibello (15 ka to present-day). Products of the Mongibello, mostly hawaiites, cover more than 80% of the present-day volcano surface (cf. Viccaro and Cristofolini, 2008 and references therein).

Previous interpretation of the Val Calanna area

At its southeastern margin, the Valle del Bove (VdB) is marked by the 1-km-wide and 2-km-long depression of Val Calanna (Figure 1B). This depression is separated from the nearby VdB by the 300-m-high steep slope of the "Salto della Giumenta" (Figures 2-3), covered by recent lava flows and bordered to the northwest by Mt. Calanna (MC; Figures 2-3), an isolated hill extending over an area of 0.7 km^2 (1325 m a.s.l.). Due to the complexity of its outcrops, mainly composed of altered agglomerates, faulted breccias and dykes, MC has been the object of contrasting interpretations. It was first attributed to remains of one of the AAC edifices (Klerkx, 1970; Romano and Sturiale, 1975; Romano and Guest 1989; Romano, 1982). Later, Mc Guire (1982) interpreted MC as the remains of a neck of a pyroclastic cone intensely intersected by dykes. In a later paper, Ferrari et al. (1989), in order to explain the origin of the faults interpreted as compressive thrust, suggested that MC could represent a portion of the pre-Etnean basement involved in regional orogenesis or, alternatively, a remnant of the early Etnean

Figure 2. Panoramic view of Val Calanna with indication of places of interest.

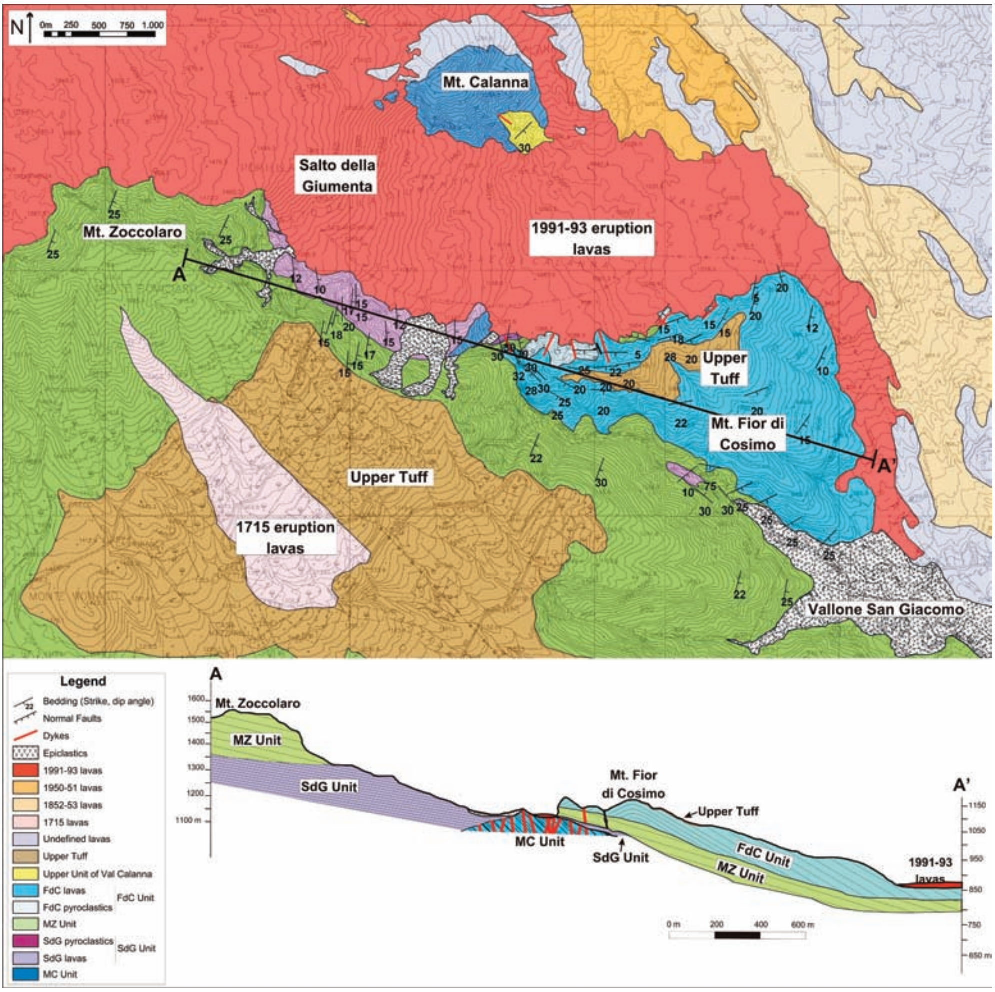

Figure 3. Geological map and stratigraphic profile of rocks outcropping in Val Calanna. Faults are all normal and the ticks are on the downthrown side.

edifice deformed by gravitational spreading. This interpretation was also adopted by Borgia et al. (1992) to support the hypothesis of gravitational spreading of the eastern flank of Mt. Etna. Recently, Ferlito and Nicotra (2010) interpreted MC as the remains of the shallower portion of the plumbing system that fed one of the AAC. Branca et al. (2008) dated its rocks at 128.7 ± 3.8 ka. To the south, the Val Calanna is bounded by the steep slopes of Mt. Zoccolaro and Mt. Fior di Cosimo (Figure 2), which constitute the southeastern corner of VdB. In this area, the Val Calanna succession has been related to two edifices belonging to different volcano-stratigraphic units (Romano, 1982; VV.AA., 1982; Ferrari et al., 1989), namely: 1) an AAC lava flow succession at the base of the northern steep flank of Mt. Zoccolaro; 2) the overlying volcanic sequence, which constitutes most of Mt. Zoccolaro and Mt. Fior di Cosimo, attributed to one of the eruptive centers of the Trifoglietto Unit. Gillot et al. (1994) dated one sample at the foot of the Mt. Fior di Cosimo escarpment at 96.0 ± 5.0 ka. This age was confirmed by Branca et al. (2008; 93.0 ± 3.0 ka) for a rock sample from the same area.

Sampling and analytical methods

The detailed geological survey of Val Calanna focused on the steep slopes of Mt. Zoccolaro, Mt. Fior di Cosimo and in the area of Vallone San Giacomo (Figure 3). Strikes and dips were measured for tectonic structures, lavas and pyroclastic levels at sites precisely determined with UTM geo-referenced coordinates by GPS (Table 1). Volcanic rock samples were also collected along the volcano-stratigraphic sections of the southern flank of Val Calanna. At Mt. Fior di Cosimo, samples were collected along a very steep, 150-m-thick, succession of lava flows. A total of 22 samples was collected at sites geo-referenced by GPS procedures (Table 2): 6 lava samples were taken from the Mt. Zoccolaro escarpment and 16 from the Mt. Fior di Cosimo area. Major elements were measured at the Dipartimento di Scienze Geologiche of the Università di Catania (Italy) using a Philips PW2404 WD-XRF on powder pellets, correcting the matrix effects according to Franzini et al. (1972). FeO concentrations were obtained by classic $KMnO_4$ titration. Loss on ignition was determined by gravimetric methods and corrected for Fe^{2+} oxidation. Major elements compositions for the mineralogical phases were measured at the Dipartimento di Scienze Geologiche of the Università di Catania (Italy) using a Tescan Vega LMU scanning electron microscope (SEM) equipped with an EDAX Neptune XM4-60 EDS micro-analyzer characterized by an ultra-thin Be window. Analyses were performed at 20 kV accelerating voltage and 0.2 nA beam current. Analyses of five phenocryst cores were performed for each mineral phase on each sample and are reported in the Electronic Supplementary Material (ESM). Precision of SEM-EDS data is in the order of 3%.

The Geology of Val Calanna

Some discrepancies were found in the existing literature for the products of the southern flank of Val Calanna. The stratigraphic position and the dips of the lavas in the Mt. Fior di Cosimo area do not correlate with the previous attribution of a more westerly-located eruptive axis (i.e. those of the Trifoglietto volcano; cf. Romano, 1982; Ferrari et al., 1989; Branca et al., 2008). Our geological survey leads to the definition of four volcano stratigraphic Units (Figure 3), informally defined from the bottom to the top of the succession as: 1) Mt. Calanna (MC); 2) Salto della Giumenta (SdG); 3) Mt. Zoccolaro (MZ); 4) Mt. Fior di Cosimo (FdC).

Mt. Calanna Unit

Products of MC Unit crop out in the northwestern portion of Val Calanna and at the foot of its southern wall, 200-m-west of the

Table 1 - Dip, GPS position (UTM) and height (a.s.l.) of volcanics products surveyed in the Val Calanna area.

#	Dip (°N)	Dip Angle	Latitude (m)	Longitude (m)	Height (m)	#	Dip (°N)	Dip Angle	Latitude (m)	Longitude (m)	Height (m)
1	45	25	2527955.033	4172904.646	755	*32*	35	15	2527855.814	4173366.394	926
2	60	25	2527807.831	4172966.626	780	*33*	25	10	2527930.589	4173645.286	916
3	64	25	2527703.240	4173059.596	817	*34*	12	12	2527887.138	4173807.973	967
4	65	25	2527600.585	4173111.892	830	*35*	345	30	2526700.333	4173703.893	1120
5	100	75	2527470.815	4173195.177	872	*36*	345	30	2526624.547	4173693.789	1151
6	50	10	2527377.845	4173164.187	838	*37*	10	30	2526654.861	4173728.145	1099
7	310	30	2527445.636	4173084.775	847	*38*	0	15	2526434.577	4173748.354	1156
8	320	30	2527540.542	4173082.839	812	*39*	355	12	2526200.651	4173814.035	1180
9	70	20	2527662.565	4173503.140	1012	*40*	355	15	2526158.211	4173746.333	1227
10	345	20	2527765.219	4173977.286	1010	*41*	360	15	2526028.870	4173893.863	1215
11	10	5	2527662.565	4173932.738	1032	*42*	5	17	2526014.724	4173871.693	1238
12	20	20	2527656.755	4173864.947	1065	*43*	0	15	2525975.315	4173846.371	1308
13	30	15	2527530.858	4173808.778	1088	*44*	15	20	2525949.043	4173816.056	1365
14	30	15	2527468.878	4173839.768	1039	*45*	17	18	2525919.739	4173785.742	1410
15	65	20	2527389.466	4173717.745	1110	*46*	10	15	2525893.466	4173746.333	1435
16	70	18	2527339.108	4173797.157	1073	*47*	5	15	2525997.546	4173621.034	1401
17	285	5	2527174.474	4173731.303	1072	*48*	10	15	2526035.944	4173652.359	1342
18	90	25	2526953.670	4173671.260	1110	*49*	10	17	2526079.394	4173694.799	1310
19	90	22	2527083.441	4173659.639	1122	*50*	355	12	2525778.272	4174006.026	1341
20	85	20	2527046.640	4173601.533	1180	*51*	350	10	2525876.288	4173962.576	1287
21	82	20	2527139.610	4173615.091	1161	*52*	25	25	2525489.781	4174179.828	1530
22	75	28	2527308.118	4173723.556	1117	*53*	20	25	2525037.087	4174279.865	1560
24	100	20	2526942.049	4173587.975	1185	*54*	20	25	2524784.973	4174116.168	1582
25	135	30	2526759.983	4173591.848	1202	*55*	45	30	2526711.934	4174573.540	1112
26	135	28	2526738.678	4173580.227	1212	*56*	20	30	2527026.212	4173184.283	1079
27	155	30	2526663.140	4173659.639	1215	*57*	22	22	2526757.930	4173287.352	1132
28	150	32	2526684.445	4173628.649	1208	*58*	10	25	2527782.778	4172691.098	795
29	120	25	2526880.069	4173537.616	1165	*59*	15	22	2527589.964	4172724.591	929
30	95	20	2527038.893	4173506.850	1109	*60*	120	25	2526849.846	4173485.787	1115
31	80	22	2527353.091	4173450.263	1059	*61*	35	15	2527285.773	4173825.907	1065

Table 2. Major element concentrations (wt%) for sampled Val Calanna rocks. FdC lavas are in order of their stratigraphic position.

Sample	**Z 2**	**Z 5**	**FDC 16**	**Z 3**	**Z 4**	**Z 6**	**FDC 11**	**FDC 4**	**FDC 13**	**FDC 3**	**FDC 1**
Unit	***SdG***	***SdG***	***SdG***	***MZ***	***MZ***	***MZ***	***FdC***	***FdC***	***FdC***	***FdC***	***FdC***
Type	lava	lava	pyro	lava	lava	lava	pyro	lava	lava	lava	lava
Latitude (m)	2527379.197	2526155.238	2526652.584	2526038.083	2526078.634	2527191.202	2526795.943	2527059.133	2527682.654	2527248.445	2527663.966
Longitude (m)	4173164.186	4173746.305	4173730.485	4173653.048	4173699.677	4173735.573	4173414.856	4173716.524	4173947.253	4173735.764	4173502.060
Altitude (m)	920	1230	1098	1360	1280	1080	1048	1086	1098	1100	1012
SiO_2	54.8	53.4	56.2	56.9	57.3	57.0	53.9	49.4	50.7	51.3	52.4
TiO_2	1.35	1.57	1.97	1.01	0.79	0.94	1.37	1.92	1.61	1.54	1.45
Al_2O_3	19.6	17.0	22.6	19.3	21.3	19.7	18.7	19.7	18.9	21.1	20.3
FeOtot	6.78	8.90	4.96	5.91	4.60	5.82	8.15	9.99	8.87	8.99	8.05
MnO	0.11	0.14	0.06	0.12	0.12	0.14	0.16	0.17	0.17	0.19	0.17
MgO	1.52	4.45	1.37	1.99	1.00	1.36	2.72	3.91	3.29	2.48	2.35
CaO	7.72	9.05	7.34	6.23	6.09	6.17	7.69	9.24	9.53	7.57	8.07
Na_2O	5.03	3.89	3.34	5.65	5.79	5.85	4.70	3.63	4.49	4.29	4.55
K_2O	2.09	1.15	1.43	2.50	2.64	2.42	1.97	1.26	1.71	1.58	1.72
P_2O_5	0.99	0.44	0.73	0.41	0.41	0.61	0.64	0.77	0.73	0.93	0.93
Total	100.0	100.0	100.0	100.0	100.0	100.0	100.0	100.0	100.0	100.0	100.0
Fe_2O_3	6.02	3.26	4.27	5.05	2.29	3.12	4.51	6.54	4.80	7.77	6.29
FeO	1.24	5.87	0.85	1.30	2.49	2.95	3.95	3.76	4.41	1.65	2.21
L.O.I.	0.99	0.14	4.86	0.53	0.39	0.40	0.84	2.38	0.68	2.96	1.31

Sample	**FDC 2**	**Z 1**	**FDC 10**	**FDC 9**	**FDC 8**	**FDC 7**	**FDC 6**	**FDC 5**	**FDC 12**	**FDC 14**	**FDC 15**
Unit	***FdC***	***FdC***	***FdC***	***FdC***	***FdC***	***FdC***	***FdC***	***FdC***	***FdC***	***FdC***	***FdC***
Type	lava	lava	lava	lava	lava	lava	lava	lava	dyke	dyke	dyke
Latitude (m)	2527590.692	2527466.846	2527528.411	2527543.802	2526793.634	2526787.478	2526778.243	2526754.387	2527315.394	2527266.145	2527016.038
Longitude (m)	4173845.114	4173185.142	4173313.659	4173409.085	4173651.112	4173634.951	4173613.403	4173571.847	4173828.111	4173799.637	4173755.722
Altitude (m)	1060	870	950	995	1180	1185	1195	1200	1045	1045	1055
SiO_2	52.6	52.4	54.1	55.6	55.9	57.0	57.6	57.0	52.3	52.4	52.1
TiO_2	1.48	1.60	1.23	1.05	1.06	0.94	0.94	1.00	1.43	1.42	1.43
Al_2O_3	20.5	19.3	20.8	20.1	19.9	19.8	19.5	19.2	20.1	20.6	19.8
FeOtot	7.95	8.29	6.51	6.72	6.59	5.94	5.84	6.29	8.41	7.15	8.70
MnO	0.15	0.18	0.14	0.15	0.14	0.15	0.14	0.15	0.18	0.16	0.20
MgO	2.00	2.22	1.64	1.46	1.37	1.30	1.25	1.45	2.17	1.64	2.27
CaO	7.94	8.21	7.32	6.25	6.23	5.90	5.91	6.15	8.34	8.44	8.45
Na_2O	4.54	4.95	5.23	5.54	5.69	5.96	5.80	5.70	4.59	5.43	4.52
K_2O	1.87	2.03	2.22	2.38	2.42	2.45	2.47	2.42	1.70	2.07	1.73
P_2O_5	0.89	0.79	0.80	0.78	0.77	0.56	0.57	0.59	0.74	0.77	0.73
Total	100.0	100.0	100.0	100.0	100.0	100.0	100.0	100.0	100.0	100.0	100.0
Fe_2O_3	4.13	3.99	3.94	4.63	5.89	5.38	5.51	5.99	4.12	2.04	4.12
FeO	4.06	4.59	2.87	2.44	1.18	1.03	0.82	0.82	4.57	5.25	4.85
L.O.I.	1.38	0.46	0.81	1.02	1.01	0.45	0.45	0.54	0.67	0.08	0.63

summit of Mt. Fior di Cosimo (Figure 3). This Unit is mostly composed of deeply altered and faulted volcanic rocks intruded by a considerable number of dykes (~ 200; Ferlito and Nicotra, 2010), which cover an area of about 0.7 km^2. Recently, Ferlito and Nicotra (2010) interpreted MC as due to the injection of a dyke swarm into older Etnean volcanic products. These dykes fed one of the AAC and its present-day outcrops could represent its shallowest portion of the volcano feeding system. Our geological survey confirmed the stratigraphic position of the MC eruptive center, which is therefore one of the most ancient volcanic centers in the VdB area belonging to the AAC.

Salto della Giumenta Unit

The Salto della Giumenta Unit (SdG) unconformably lies over the MC (Figure 3). SdG products crop out at the base of the Mt. Zoccolaro escarpment from the higher sector of the steep "Salto della Giumenta" (~ 1400 m a.s.l.) to the foot of Mt. Fior di Cosimo (~ 1100 m a.s.l.), with a maximum thickness of 80 m. The bulk of this Unit is constituted by a succession of lava flows (1-3 m thick) exhibiting a constant plunge (N90°E) and dip angle of 15-20°. At the top and in conformity with this lava flow succession, a pyroclastic deposit dipping N85°E at an angle of 30° was found. Three different levels were recognized in this succession (Figure 4): Level A) the basal layer is composed only of light yellow and finely layered tuffs with no lithics; Level B) the middle layer is a matrix supported breccia, mostly made up of angular decimeter-sized, unsorted lithic blocks in a yellowish and fine-grained juvenile ash; Level C) the uppermost level is similar to Level B, and differs only in the smaller size of the lithics. This deposit is here interpreted as originated by a pyroclastic flow related to the last stage of activity at the SdG Center. The top of this sequence, cut by an erosional surface, is overlain by a chaotic layer of angular, decimetric lithic blocks in an unsorted matrix, which is interpreted as a lahar deposit (Figure 4). On the whole, products of the SdG Unit would be related to the earlier activity of a center belonging to AAC (Romano, 1982) with its main eruptive axis located west of Mt. Zoccolaro.

Mt. Zoccolaro Unit

Volcanic products of this Unit (MZ) directly overlie the SdG lahar deposit and constitute most of the Mt. Zoccolaro ridge, from an elevation of ~ 1700 m a.s.l. in the western part down to ~ 700 m a.s.l. in the eastern sector (Figure 3). MZ was considered distinct from SdG given that its deposits lie in unconformity above the lahar at the SdG top. Also, the thickness of the MZ lavas (15-20 m) is ten times that of the SdG lavas (1-3 m).

MZ products crop out in a well-exposed section on the southern flank of Val Calanna below Mt. Zoccolaro and in the deep gully of Vallone San Giacomo (Figure 3). The MZ Unit is composed of a 250/300-m-thick sequence of lava flows generally plunging easterly with a dip angle of 20°. These flow units are continuous across the Vallone San Giacomo, providing evidence that no tectonic structures were active in this area after the MZ succession emplacement. On the opposite flank of the valley, lava flows crossing the Vallone San Giacomo from its southern walls dip under the volcanic succession of Mt. Fior di Cosimo, which in turn plunges southward (see below). Furthermore, at the foot of the northern flank of Mt. Fior di Cosimo (Figure 3), a thick lava flow was found which is very similar to the MZ lavas and different from the overlying products of Mt. Fior di Cosimo. This lava flow (sample Z6) dips toward NE, with opposite plunge with respect to the overlying succession (Figure 3). It corresponds to the FC lava flow sample dated at 93 ± 3 ka (Gillot et al., 1994; Branca et al., 2008), and was here attributed to the MZ Unit.

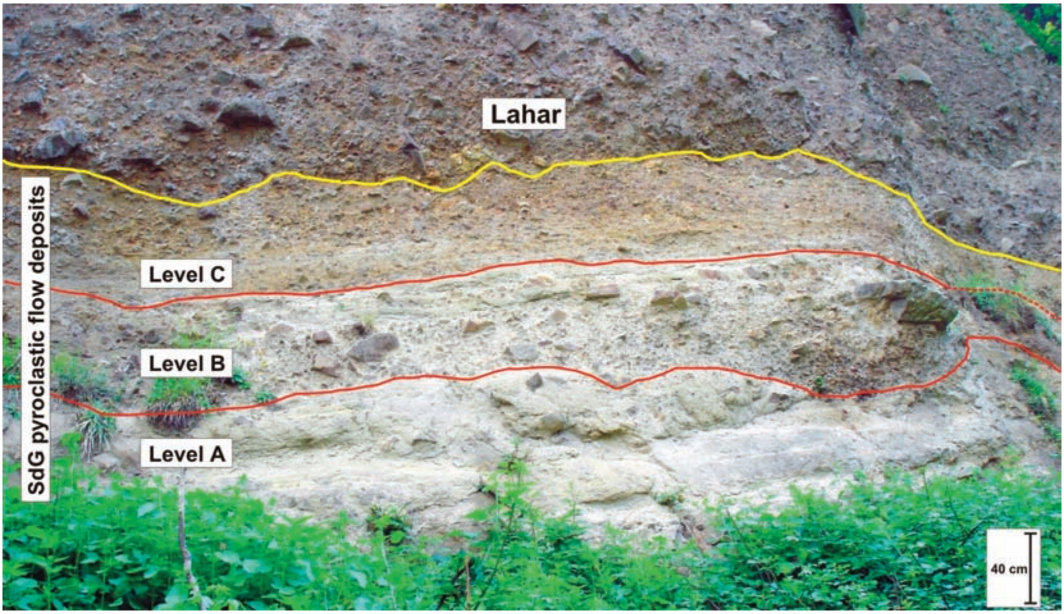

Figure 4. Pyroclastic flow and lahar deposits at the top of the Salto della Giumenta Unit. The former is made up of three levels with differing structure and abundances of primary/lithic products.

Fior di Cosimo Unit

The remains of the edifice of the FdC eruptive center consist of a ~ 150-m-thick succession of lava flows and tephra, which chiefly crops out at the ridge between Val Calanna and Vallone San Giacomo (Figure 3). FdC Unit unconformably overlaps the uppermost MZ levels and is mantled at its top by the "Upper Tuffs" (Romano, 1982) dated at ~ 8 ka by Gillot et al. (1994). The FdC Unit is distinct from the underlying MZ, as evidenced by: 1) the opposite plunge and the different volcanological s.l. features of the MZ lava flow at the base of the central portion of Mt. Fior di Cosimo with respect to the overlying lava flows; 2) the unconformable attitude of some FdC lavas that overlie MZ products with an opposite plunge in the Vallone San Giacomo; 3) different geochemical compositions (see next Section).

Pyroclastic deposits are found only in the central portion of the lava flow sequence along the northern flank of Mt. Fior di Cosimo (1050 m a.s.l.), and at the base of the succession between 1080 and 1170 m in the western area. The first outcrop is constituted by a 8-m-thick well-stratified bed of coarse ash, highly vesiculated lapilli and fuse-shaped bombs (with bubbles up to 1 cm across), plunging N100°E with a dip angle of 30° (Figure 3; Table 1). These pyroclastic levels are cut by two thin dykes N-S and E-W oriented, which are considered to be related to the FdC feeding structures. All these features allow this pyroclastic level to be interpreted as very proximal (< 300 m) deposits. The western basal outcrop of tephra plunges N180°E and is composed of a 50-m-thick succession of alternating ashes, lapilli and bomb beds, interpreted as pyroclastic fall levels, interlayered with a few thin (up to 50 cm) lava flows (Figure 5B). This succession is cut by two vertical dykes striking N170°E and N30°E, and by a N175°E directed normal fault dipping 65° with a measured offset of ~ 2 m.

One of the particular characteristics of the FdC lava flows is their dip, which ranges over the entire azimuth angle between SW and E. In addition, the overall thickness of the succession and the number of flow units decrease laterally away from the summit of Mt. Fior di Cosimo. To the west, six lava flows dipping SW are attributed to this Center (Figure 3; Table 1). In the central portion of FdC, 15 lava flows constitute the maximum thickness of the succession, showing a southerly dip (Figure 3; Table 1). In the FdC eastern portion, lava flows plunge between E and SE and the overall thickness of the succession decreases toward the southern- and easternmost areas. These observations suggest that lava flows are radial with respect to an eruptive axis located at the center of the Val Calanna and are consistent with the idea that FdC is distinct from the older MZ Unit.

Whole rock chemistry

Major element concentrations for the collected samples are reported in Table 2. Following IUGS recommendations for the classification of volcanic rocks, only rocks having L.O.I. < 2 wt% have been plotted in the Total Alkali - Silica (TAS; Figure 6A; Le Maitre, 2002) diagram. Products that crop out in the Val Calanna area exhibit a wide compositional variability from

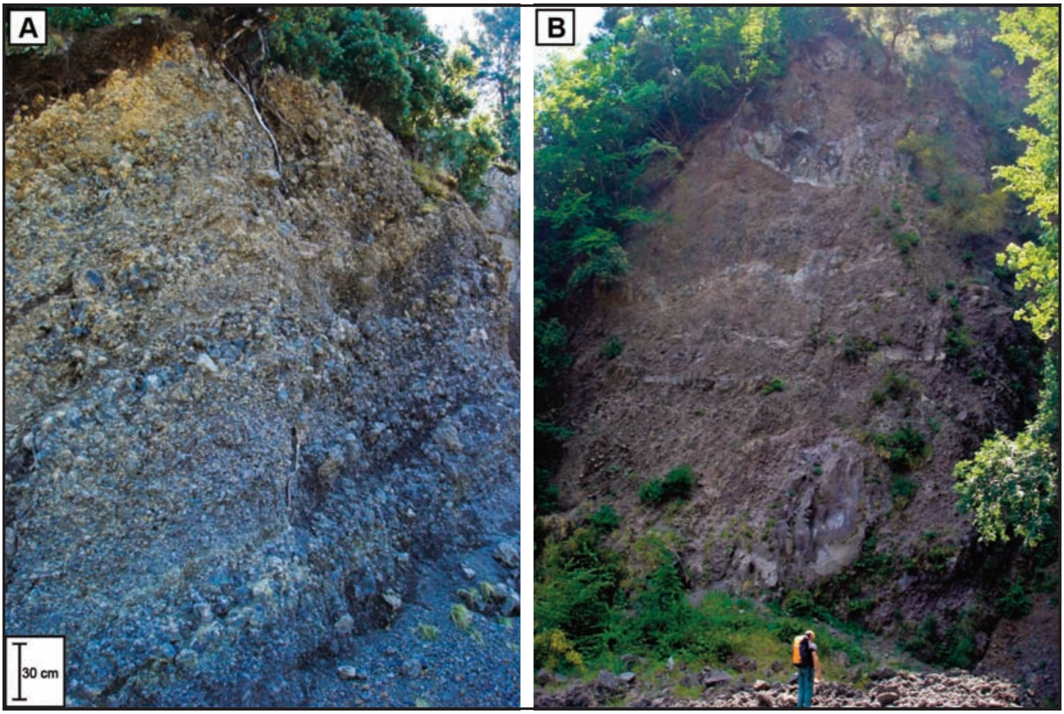

Figure 5. A) Pyroclastics deposit formed by welded scoriae and lapilli outcropping in the eastern part of Mt. Fior di Cosimo; B) Alternation of abundant pyroclastic products and lavas in the central portion of the Mt. Fior di Cosimo.

basalts to benmoreites, i.e. a typical Etnean alkaline sequence of differentiation (Tanguy et al., 1997). SdG samples show a scattered distribution in the TAS diagram (Figure 6A), as one sample plots in the mugearite field whereas the other two, showing an alkali depletion, fall into the basaltic andesite field. The three MZ lavas, very similar in composition, plot in the benmoreite field (Figure 6A). Major elements of the FdC Unit (lava, tephra and dykes) plot along a well-defined trend from basalt to benmoreite (Figures 6A-7). Figure 7 shows the widely ranging values of SiO_2 and MgO (49.4-57.6% and 1.25-3.91 wt% respectively), with the other oxides that present fairly good negative or positive correlations with respect to SiO_2 (Figure 7; Table 2). In addition, the detailed stratigraphically-controlled sampling on the FdC Unit allowed the plot of chemical compositions as a function of their stratigraphic position (Figure 8). These diagrams show a positive correlation between stratigraphic position (from bottom to top) and the degree of differentiation of lavas (Figure 8). FdC compositions were compared with data from Cristofolini et al. (1991) which refer to products of the ancient Etnean volcanic phases (Figure 6B-C). SiO_2 and TiO_2 show a negative correlation, very similar to that observed for the Trifoglietto volcanics, where the TiO_2 depletion in the more differentiated products has been related to amphibole fractionation (Figure 6B; e.g., Cristofolini, 1971; Cristofolini et al., 1991; Viccaro et al., 2007). However, the K_2O vs P_2O_5 diagram (Figure 6C) evidences that FdC volcanics have higher P_2O_5 and lower K_2O compared to the typical values of Trifoglietto products.

Petrography and Mineral Chemistry

The petrographic features of the samples conform to those of typical Etnean volcanics (Cristofolini et al., 1991; Tanguy et al., 1997; Viccaro and Cristofolini, 2008). All the lava

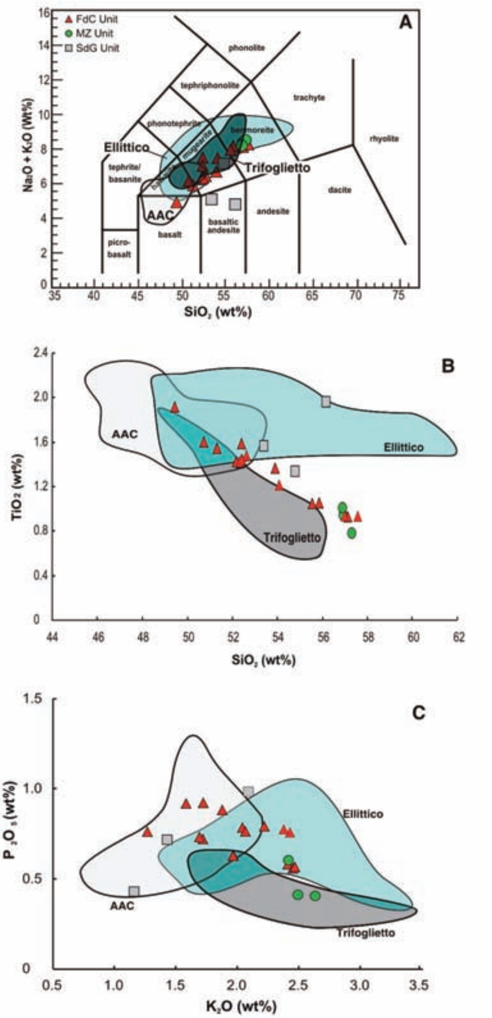

Figure 6. A) Total Alkali Silica (TAS; Le Maitre, 2002) of Val Calanna volcanic rocks; fields for the Ancient Alkaline Centers (AAC), Trifoglietto and Ellittico are taken from Cristofolini et al., 1991. B) SiO_2 vs TiO_2 diagram of rocks of Val Calanna compared with the compositional fields of AAC, Trifoglietto and Ellittico (dataset of Cristofolini et al., 1991); FdC lavas present a geochemical behavior similar to those of Trifoglietto. C) K_2O vs. P_2O_5 diagram of Val Calanna volcanics (fields from Cristofolini et al., 1991); SdG lavas present a signature similar to those of the AAC, the MZ lavas to those of the Trifoglietto, whereas the FdC lavas plot both on the AAC and Ellittico fields.

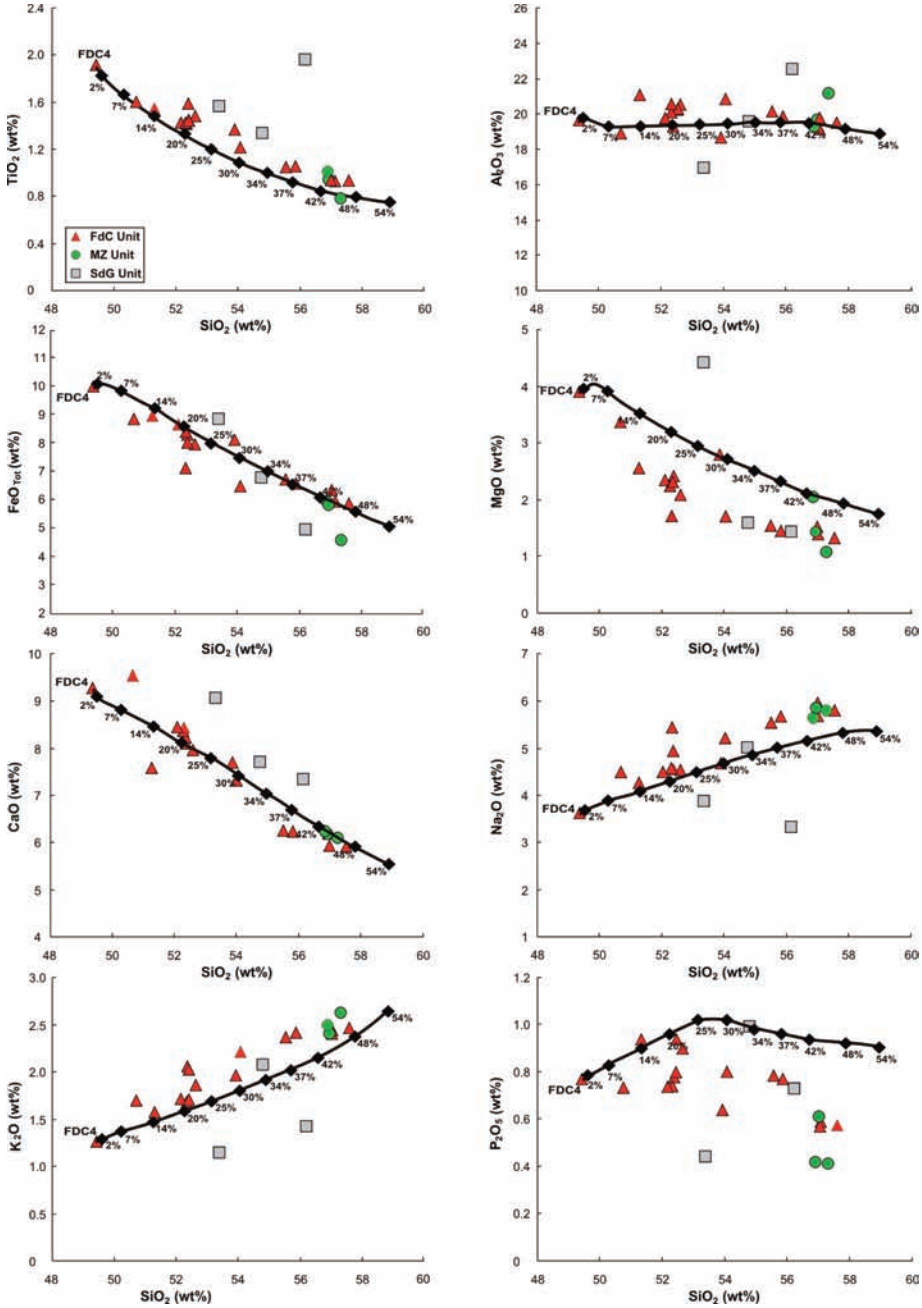

Figure 7. SiO_2 vs major elements diagrams of Val Calanna volcanic rocks. The crystal fractionation trends obtained through the MELTS simulation starting from a FdC4-like magma are shown with percentages of fractionation. See discussion for explanation.

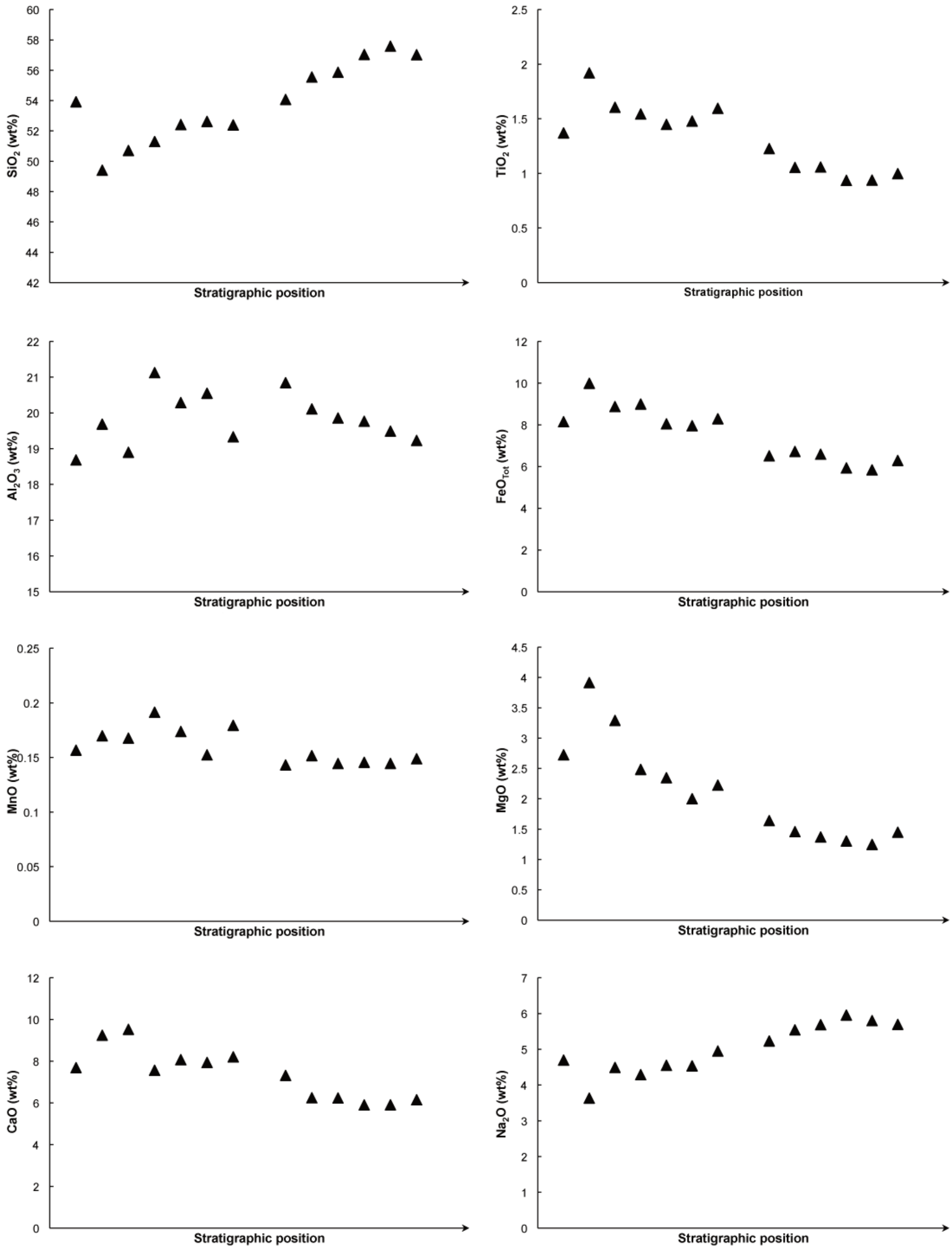

Figure 8. Major element compositions of FdC lavas vs the stratigraphic position derived from geological survey. The bottom of the succession is at left of each diagram.

samples collected from Val Calanna are porphyritic with P.I. (Porphyricity Index in vol%) between 15 and 30. Plagioclase, clinopyroxene and olivine in varying proportions usually make up about 85-95 vol% of total phenocrysts. Opaque oxides (Ti-magnetite; < 5 vol%) and apatite (< 2 vol%) complete the phenocryst assemblage. Amphibole (< 3 vol%) was only found as megacrysts in MZ lavas and in FdC lavas of the higher stratigraphic positions. The groundmass is mesocrystalline and mostly displays intersertal and pylotaxitic textures, with the latter found only in the most differentiated products of the three eruptive Centers considered. Minerals in the groundmass are commonly plagioclase (65-75 vol%), clinopyroxene (< 20 vol%), olivine (< 5%) and Ti-magnetite (< 5%). Glomerophyric structures, up to 5 mm across and composed of all the constituting minerals (Figure 9), are present only in the most differentiated products of FdC. Textural relationships indicate olivine and Ti-magnetite as the first crystallizing phases, followed in turn by clinopyroxene, plagioclase and, when they occur, amphibole and/or apatite.

Plagioclase is the most abundant phase in all the collected samples. Phenocrysts are from euhedral to subhedral with sizes ranging between 3 and 7 mm in products from all the eruptive centers. Microanalysis for major oxides was performed at the plagioclase crystal cores. Measured compositions are reported in the ESM together with structural formulae calculated on the basis of 8 oxygens. Compositions cover a wide spectrum, from andesine to bytownite (Figure 10A; ESM). Plagioclase compositions of the SdG lavas (mugearite-benmoreite) range between An_{47} and An_{57}, whereas those of MZ (benmoreite) display a wider compositional range between An_{36} and An_{66} (Figure 10A; ESM). Plagioclases of the FdC lavas show a significant decrease in the An content (from $\sim An_{82}$ down to $\sim An_{36}$) of their cores from the bottom to the top of the volcanic succession (Figure 11).

Clinopyroxene is the most abundant mafic phase; medium-sized (1-7 mm) and pale-green in color very similar to other pyroxenes of the Etnean alkaline suite (cf. Nazzareni et al., 2003). Measured compositions of clinopyroxene phenocryst cores are reported in the ESM along with structural formulae calculated on the basis of 6 oxygens. Compositions range from the diopside to augite fields in the QUAD diagram

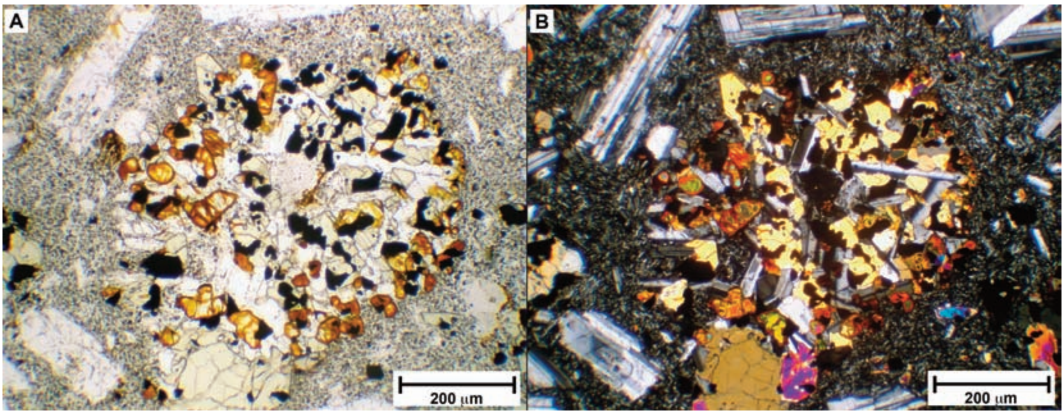

Figure 9. Plane (A) and cross (B) light polarized images of a glomerophyric structure in the last-emitted products of FdC Unit.

(Figure 10B) and can be defined as "Ti-bearing" Al-Fe^{3+}- augite and Al-Fe^{3+}- diopside (Morimoto et al., 1988). Mg# values [calculated as Mg /(Mg +Fe^{2+})] were plotted against stratigraphic position to emphasize possible variations through time (Figure 11). In this regard, no clear variations are observed, as the median values remain fairly constant through the whole FdC volcanic succession (Figure 11).

Olivine is generally present as medium-sized (1-5 mm) euhedral to subhedral phenocrysts. The crystals display a brown-reddish iddingsitic rim

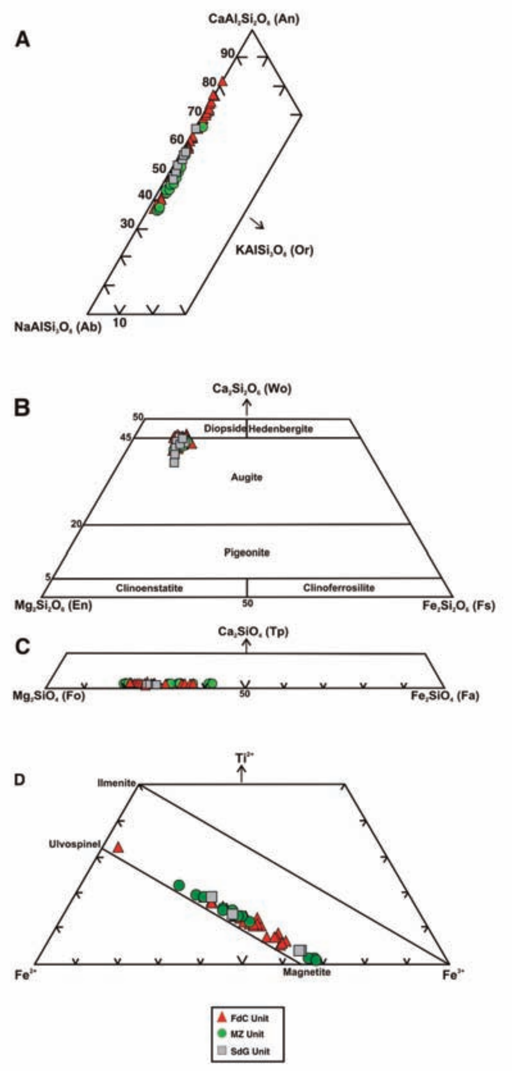

Figure 10. Compositional variation of the mineral phases of Val Calanna succession: A) plagioclase crystals; B) clinopyroxene crystals; C) olivine crystals; D) opaque oxides.

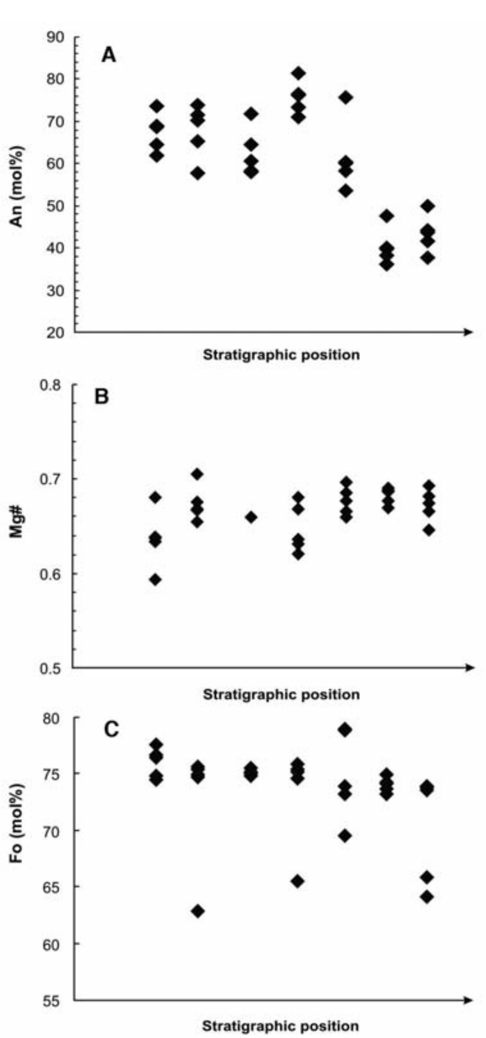

Figure 11. Compositional variation of the mineral phases of Mt. Fior di Cosimo plagioclase (A), clinopyroxene (B) and olivine (C) related to the stratigraphic position of lava samples.

in the FdC lavas, indicating that these products underwent some degree of alteration. Measured major oxide compositions are reported in the ESM along with structural formulae calculated on the basis of 4 oxygens. Compositions are quite variable among the Centers considered, with forsterite contents varying from Fo_{58} to Fo_{78} (Figure 10C; ESM). FdC olivine phenocrysts show a slight trend to more fayalitic compositions only at the top of the volcanic succession (Figure 11), although compositions are generally scattered within the succession.

Opaque oxides are generally present as small-sized (0.1-1 mm) euhedral to anhedral phenocrysts, and are frequently enclosed in olivine and clinopyroxene phenocrysts, suggesting their early crystallization. Measured major oxide compositions and structural formulae, calculated on the basis of 4 oxygens, are reported in ESM. Opaque oxides can be classified as Ti-magnetite (ESM; Figure 10D).

Apatite is found either as 300-mm-long prismatic and colorless phenocrysts (< 1% vol.), often enclosed in clinopyroxene and plagioclase crystals, or in the groundmass.

Amphibole occurs as phenocrysts in benmoreites, specifically in all the MZ sampled rocks and at the top of FdC succession (Figure 12). In the MZ lavas, they are 2-8 mm long (Figure 12A), whereas exclusively small-sized crystals (< 1 mm) occur in the FdC Center (Figure 12B). Amphibole crystals are euhedral, brown in color, markedly pleochroic with α' pale yellowish brown and γ' dark brown, and c^γ angles < 10° (Figure 12). The optical features conform with those of the calcic amphiboles (kaersutite-pargasite-Mg-hastingsite), already found within the Etnean succession (Viccaro et al., 2007 and references therein). Amphibole phenocrysts always show a dark and opaque breakdown rim, indicating disequilibrium with the hosting melt (cf. Viccaro et al., 2007).

Discussion

Volcanological succession of the Val Calanna area

Starting from the bottom of the succession, our survey confirmed that MC Unit is the lowermost of the Val Calanna area and, more in general, of the VdB. This eruptive center now crops out only as a small portion of a dykes swarm, deeply faulted and geochemically altered, which can be attributed to the AAC (Ferlito and Nicotra, 2010). After the end of its activity, the eruptive center of MC was deeply eroded, with volcanic

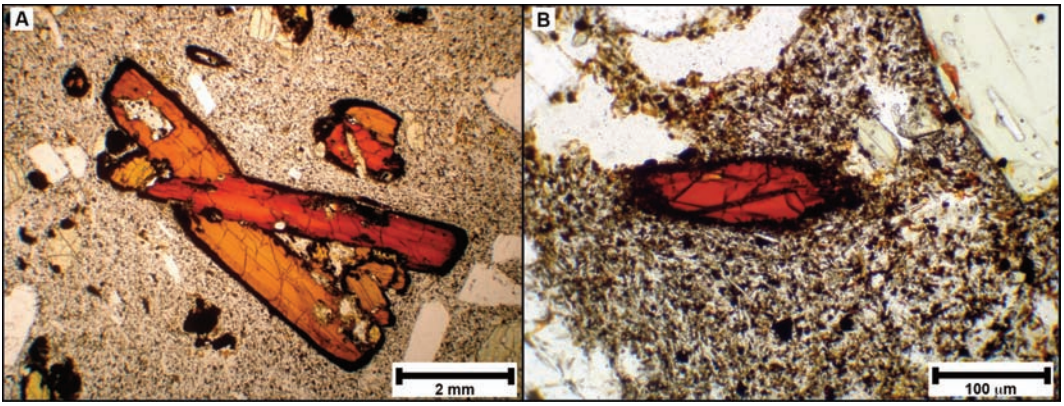

Figure 12. Amphibole crystals in Monte Zoccolaro lavas (A) and in one of the last-emitted lavas of Mt. Fior di Cosimo Center (B).

and most of the sub-volcanic products swept away (cf. Ferlito and Nicotra, 2010).

Above the MC Unit, the volcanic succession of Val Calanna (Figure 3) is more complex than previously proposed (Romano, 1982; Ferrari et al., 1989; Branca et al., 2008). In particular, two volcano-stratigraphic Units (SdG and MZ) were recognized at the Mt. Zoccolaro ridge.

Due to the particular characteristics of the very limited outcrops of SdG Unit products, it is not possible to identify the exact location of the main eruptive axis of the SdG eruptive center but, due to the dip of its products, it could be located W of the Mt. Zoccolaro summit (Figure 3). On the grounds of its position within the volcano-stratigraphic succession on the southern rim of Valle del Bove (cf. Romano, 1982; Ferrari et al., 1989; Calvari et al., 1994) and its geochemical signature, the SdG eruptive center should belong to the AAC (by Romano, 1982) or to the VB phase (Branca et al., 2008). In all likelihood, its activity might be related to an eruptive center, named “Tarderia” volcano, firstly recognized on the basis of morphological evidence (Romano and Guest, 1979; Cristofolini et al., 1982). After the last and very explosive phases of the SdG eruptive center, testified by pyroclastic flow deposits, part of the edifice was eroded, covered by lahar deposits and unconformably overlain by products of the MZ eruptive center. Considering that SdG products directly overlie those of the MC in the southern wall of Val Calanna outcrop, on the basis of its attribution inferred here and of the $^{40}Ar/^{39}Ar$ dating of the “Tarderia” Center to ~ 106 ka (Branca et al., 2008), the period of time between the end of MC Center activity and the emplacement of the first overlaying lavas would therefore be ~ 22 ka.

The 300-m-thick succession of the MZ Unit crops out along the southern ridge of Val Calanna as the relic of a large edifice that, according to the constant easterly dips of its lavas, had its westernmost eruptive axis located within the Valle del Bove. This eruptive center was deeply eroded before the onset of the FdC activity, as testified by the contact of FdC lavas over the deeply denudated surface of MZ products. The thick lava flows of this eruptive center have benmoreitic composition and low TiO_2 content (~ 1 wt%; Figure 6B-C). These low TiO_2 values for such differentiated products might be explained by fractionation of Ti-rich phases, such as Ti-magnetite during the early stage of crystallization and titanium-rich amphibole during the late ones (cf. Cristofolini, 1971; Cristofolini et al., 1991). During such late stages of magma evolution, ratios among all the major elements except titanium remain fairly constant if amphibole is fractionated from the system, since the amphibole composition is not greatly dissimilar to that of the melt. TiO_2 depletion, together with the K_2O and P_2O_5 concentrations (Figure 6B-C) make the MZ products similar to those of the Trifoglietto Center (Romano, 1982; Cristofolini et al., 1982).

According to the volcanic succession proposed here, the eroded MZ Unit is overlain by a 150-m-thick succession of lavas, pyroclastic and epiclastic deposits in the Mt. Fior di Cosimo area (Figure 3). These are remnants of the activity of a small eruptive center, not previously recognized, named here as “Fior di Cosimo” (FdC), which was surely active in the Val Calanna between 93 ± 3 ka and 8 ka (the ages, respectively, of the MZ lava at the bottom and the “Upper Tuff” at the top; Romano, 1982; Branca et al., 2008 and references therein). Field observations in the Vallone San Giacomo indicate that the FdC edifice grew over the deeply abraded surface of the MZ Center and, after the end of its activity, underwent important processes of erosion. Indeed, although the thickness of the succession of this eruptive center (~ 150 m) is presumably fully preserved, the northern portion of the FdC edifice has been involved in the deep erosional processes affecting the VdB. As a consequence, it was swept away leaving a steep ENE-WSW escarpment 100-m-high that now constitutes the southeastern termination of the rim of the Valle del Bove (Figures 3-4).

Magma evolution of the Fior di Cosimo eruptive center

The major element variability observed for volcanic rocks of the FdC Unit follows trends that can be ascribed to a liquid line of descent (Figure 7). This trend is also strictly related to time, as the last emitted volcanics are the most differentiated. In order to verify this inference, a simulation of crystal fractionation was performed through the MELTS code (Ghiorso and Sack, 1995; Asimov and Ghiorso, 1998). Simulation starts from the most mafic and less porphyritic FdC basalt (FdC4 sample; Table 2), which is also the lowermost lava in the succession under examination. The FdC4 sample cannot be considered a primary magma (SiO_2 = 49.4 wt%; MgO = 3.91 wt%; Table 2), but it could represent a poorly differentiated magma after a first step of fractionation at depth of olivine, Fe-Ti-oxides and clinopyroxene (cf. Cristofolini and Romano, 1982). Parameters used for the simulation are: T ranging from 1100 to 980 °C; P = 100 MPa; fO_2 at the QFM buffer; the original H_2O content was set at 2.3 wt%. The T range is in accordance with the Etnean magmatic temperatures (cf. Cristofolini et al., 1987). In this way, the MELTS software simulates the cooling of the magma body as differentiation proceeds. The constant P value simulates residence of the FdC4 magma at about 4 km b.s.l. (considering density of the host-rock of 2800 kg/m^3; Corsaro and Pompilio, 2004). The H_2O content and the fO_2 values are in agreement with values measured by Métrich et al. (1993) for Etnean magmas crystallizing at shallow depth and with the calculation of D'Orazio et al. (1998) for Ellittico magmas. Under these conditions, the most evolved FdC compositions can be explained by the fractionation of a mineral assemblage consisting of 32% of ~ An_{66-82} plagioclase, 8% of augitic clinopyroxene, 8 wt% of spinel, 4% of ~ Fo_{68-72} olivine and traces (< 1%) of apatite from a FdC4-like basaltic composition (54% of total solid fractionated; Figure 7).

Crystal fractionation simulation therefore shows that the compositional variability of the FdC volcanic rocks represents a liquid line of descent. The only exception is represented by the calculated MgO trend (Figure 7), which matches that of a FdC dyke, but is higher than the measured FdC lava compositions. Such variations can be explained by assuming a higher amount of olivine fractionation than that resulting from the MELTS simulation. The CaO and P_2O_5 depletion can be due to a larger fractionation of apatite, whereas Na_2O enrichment can be explained by the accumulation of evolved plagioclase. Enrichment/depletion may have occurred in the very final stages of crystallization in the groundmass during the syn-eruptive phases, a process that MELTS is not able to reproduce. Due to the limits of MELTS for hydrous phases, amphibole crystallization is not reproduced; this may also be the cause of anomalies in the trend of some oxides, especially for the most evolved products.

Inferences regarding the geometry of the FdC shallow feeding system might be provided through a time-integrated analysis of the compositional variability (Figure 8). Once the FdC4-like magma intruded at shallow levels of the Etnean crust (~ 4 km), a small-sized magma reservoir formed and then underwent fractionation of olivine, clinopyroxene and Fe-Ti-oxides. The occurrence of cumulates with this assemblage (except for the first-emitted lavas) lends weight to this hypothesis. During the second stage of the FdC magmatic evolution, a shift towards more differentiated terms occurred (Figure 8). This may suggest that magma supply from the deeper portions of the Etnean feeding system ceased, leading to further differentiation via crystal fractionation of the residing magmas (up to 54%

of minerals subtracted). This favored the gradual increase of the total volatile pressure within the system, which in turn allowed the crystallization of Ti-rich amphibole such as kaersutite, as observed in the last-emitted products.

All the available data suggests that FdC could be ascribed to a pre-Ellittico volcanic phase in which small-sized eruptive centers developed in the Val Calanna area. This hypothesis agrees with the occurrence of several minor eruptive centers also found by Lopez et al. (2006) in the northeastern wall of the Valle del Bove within the same time interval (102-80 ka).

Acknowledgements

We would like to express our gratitude to Elisabetta Giuffrida for her technical assistance in the analysis of major elements for the whole rock. Antonio Gianfagna, Alessandro Tibaldi and Massimo Coltorti are greatly acknowledged for the editorial assistance as well as for having critically revised the early-submitted version of the manuscript providing constructive comments and suggestions. This work has been supported by grant to Renato Cristofolini from the University of Catania. We would also like to thank Mike Wilkinson for his help with the English version of this paper.

References

Asimow P.D. and Ghiorso M.S. (1998) - Algorithmic modifications extending MELTS to calculate subsolidus phase relations. *American Mineralogist*, 83, 1127-1131.

Borgia A., Ferrari L. and Pasquarè G. (1992) - Importance of gravitational spreading in the tectonic and volcanic evolution of Mount Etna. *Nature*, 357, 231-235.

Branca S., Coltelli M. and Groppelli G. (2004) - Geological evolution of Etna volcano. In: Bonaccorso A., Calvari S., Coltelli M., Del Negro C., Falsaperla S. (eds) - Mt. Etna Volcano Laboratory. AGU (*Geophysical Monograph Ser*ies), 143, 49-63.

Branca S., Coltelli M., De Beni E. and Wijbrans J. (2008) - Geological evolution of Mount Etna volcano (Italy) from earliest products until the first central volcanism (between 500 and 100 ka ago) inferred from geochronological and stratigraphic data. *International Journal of Earth Science*, 97, 135-152.

Calvari S., Groppelli G. and Pasquarè G. (1994) - Preliminary geological data on the south-western wall of the Valle del Bove, Mt. Etna, Sicily. *Acta Vulcanologica*, 5, 15-30.

Coltelli M., Garduño V.H., Neri M., Pasquarè G. and Pompilio M. (1994) - Geology of the northern wall of the Valle del Bove, Mt. Etna (Sicily). *Acta Vulcanologica*, 5, 55-68.

Corsaro R.A. and Cristofolini R. (1997) - Geology, geochemistry and mineral chemistry of tholeiitic to transitional Etnean magmas. *Acta Vulcanologica*, 9, 55-66.

Corsaro R.A. and Pompilio M. (2004) - Buoyancy-controlled eruption of magmas at Mt. Etna. *Terra Nova*, 16, 16-22.

Cristofolini R. (1971) - La distribuzione del titanio nelle vulcaniti etnee. *Periodico di Mineralogia*, 40, 41-66.

Cristofolini R. and Romano R. (1982) - Petrologic features of Etnean volcanic rocks. *Memorie della Società Geologica Italiana*, 23, 99-115.

Cristofolini R., Patanè G. and Recupero S. (1982) - Morphologic evidence for ancient volcanic centers and indications of magma reservoirs underneath Mt. Etna, Sicily. *Geografia Fisica e Dinamica del Quaternario*, 5, 3-9.

Cristofolini R., Corsaro R.A. and Ferlito C. (1991) - Variazioni petrochimiche nella successione etnea: un riesame in base a nuovi dati da campioni di superficie e da sondaggi. *Acta Vulcanologica*, 1, 25-37.

Cristofolini R., Menzies M.A., Beccaluva L. and Tindle A. (1987) - Petrological notes on the 1983 lavas at Mount Etna, Sicily, with reference to their REE and Sr-Nd isotope composition. *Bulletin of Volcanology*, 49, 599-607.

D'Orazio M., Tonarini S., Innocenti F. and Pompilio M. (1997) - Northern Valle del Bove volcanic succession Mt. Etna, Sicily: petrography, geochemistry and Sr-Nd isotope data. *Acta Vulcanologica*, 9, 8-16.

D'Orazio M., Armienti P. and Cerretini S. (1998) - Phenocryst/matrix trace-element partition coefficients for hawaiite-trachyte lavas from the

Ellittico volcanic sequence (Mt. Etna, Sicily, Italy). *Mineralogy and Petrology*, 64, 65-88.

Ferlito C. and Cristofolini R. (1989) - Geologia dell'area sommitale dell'Etna. *Bollettino Accademia Gioenia di Scienze Naturali*, 22, 357-380.

Ferlito C. and Cristofolini R. (1991) - Evidenze di corpi subvulcanici poco profondi nella successione etnea lungo le pareti occidentali della Valle del Bove. *Memorie della Società Geologica Italiana*, 47, 485-493.

Ferlito C. and Nicotra E. (2010) - The dyke swarm of Mount Calanna (Etna, Italy): an example of the uppermost portion of a volcanic plumbing system. *Bulletin of Volcanology*, 72, 1191-1207.

Ferrari L., Calvari S., Coltelli M., Innocenti F., Pasquarè G., Pompilio M., Vezzoli L. and Villa I. (1989) - Nuovi dati geologici e strutturali sulla Valle di Calanna, Etna: implicazioni per l'evoluzione del vulcanismo etneo. *Bollettino GNV*, 2, 849-860.

Ghiorso M.S. and Sack R.O. (1995) - Chemical mass transfer in magmatic processes 4. A revised and internally consistent thermodynamic model for the interpolation and extrapolation of liquid-solid equilibria in magmatic systems at elevated temperatures. *Contribution to Mineralogy and Petrology*, 119, 197-212.

Gillot P.Y., Kieffer G. and Romano R. (1994) - The evolution of Mount Etna in the light of potassium-argon dating. *Acta Vulcanologica*, 5, 81-87.

Klerkx J. (1970) - La caldeira de la Valle del Bove: sa signification dans l'evolution de l'Etna. *Bulletin of Volcanology*, 34, 726-737.

Lanzafame G. and Vestch P. (1985) - Les dykes de la Valle del Bove (Etna, Sicile) et le champ de constraints régionales. *Revue de Géographie Physique et de Gèologie Dynamique*, 26, 147-156.

Le Maitre R.W. (2002) - A classification of igneous rocks and glossary of terms. Cambridge University Press.

Lopez M., Pompilio M. and Rotolo S.G. (2006) - Petrology of some amphibole-bearing volcanics of the pre-Ellittico period (102-80 ka), Mt. Etna. *Periodico di Mineralogia*, 75, 151-170.

Mc Guire W.J. (1982) - Evolution of the Etna volcano: information from the southern wall of the Valle del Bove. *Journal of Volcanology and Geothermal Research*, 13, 241-271.

Métrich N., Clocchiatti R. and Mosbah M. (1993) - The 1989-90 activity of Etna. Magma mingling and ascent of a H_2O-Cl-S rich basaltic magma. Evidence for the phenocrysts melt inclusions. *Journal of Volcanology and Geothermal Research*, 59, 131-144.

Monaco M., Tapponier P., Tortorici L. and Gillot P.Y. (1997) - Late Quaternary slip rates on the Acireale-Piedimonte normal faults and tectonic origin of Mt. Etna (Sicily). *Earth and Planetary Science Letters*, 147, 125-139.

Monaco C., Catalano S., Cocina O., De Guidi G., Ferlito C., Gresta S., Musumeci C. and Tortorici L. (2005) - Tectonic control on the eruptive dynamics at Mt. Etna volcano (Sicily) during the 2001 and 2002-03 eruptions. *Journal of Volcanology and Geothermal Research*, 144, 211-233.

Monaco C., De Guidi G. and Ferlito C. (2010) - The Morphotectonic map of Mt. Etna. *Italian Journal of Geosciences*, 129, 408-428.

Morimoto N., Fabries J., Ferguson AK., Ginzburg I.V., Ross M., Seifert F.A., Zussmann J., Aoki K. and Gottardi G. (1988) - Nomenclature of pyroxenes. *American Mineralogist*, 73, 1123-1133.

Nazzareni S., Busà T. and Cristofolini R. (2003) - Magmatic crystallization of Cr-Al diopside and Al-Fe^{3+} diopside from the ancient alkaline basalts (Mt. Etna, Sicily). *European Journal of Mineralogy*, 15, 81-93.

Nicotra E. (2010) - Genesis and differentiation of ancient Mt. Etna magmas (Ellittico volcano, 45-15 ka): a multidisciplinary approach from geology to melt inclusions. *Plinius*, 36, 169-177.

Romano R. and Guest J.E. (1979) - Volcanic geology of the summit and northern flank of Mount Etna, Sicily. *Bollettino della Società Geologica Italiana*, 98, 189-215.

Romano R. (1982) - Succession of the volcanic activity in the Etnean area. *Memorie della Società Geologica Italiana*, 23, 27-48.

Sartorius v. Waltershausen W. (1880) - Der Aetna. Leipzig, 2 volumes, 371 + 548 pp.

Tanguy J.C., Condomines M. and Kieffer G. (1997) - Evolution of the Mount Etna magma: Constraints on the present feeding system and eruptive mechanism. *Journal of Volcanology and Geothermal Research*, 75, 221-250.

Viccaro M., Ferlito C. and Cristofolini R. (2007) - Amphibole crystallization in the Etnean feeding system: mineral chemistry and trace element partitioning between Mg-hastingsite and alkali basaltic melt. *European Journal of Mineralogy*, 19, 499-511.

Viccaro M. and Cristofolini R. (2008) - Nature of mantle heterogeneity and its role in the short-term geochemical and volcanological evolution of Mt. Etna (Italy). *Lithos*, 105, 272-288.

VV. AA. (1982) - Carta Geologica del Monte Etna, Scala 1:50.000. *Memorie della Società Geologica Italiana*, 23.

Submitted, January 2011 - Accepted, May 2011